Multicellular PD Control in Microbial Consortia

Vittoria Martinelli, Davide Salzano, Davide Fiore, Mario di Bernardo

***Abstract*— We propose a multicellular implementation of a biomolecular PD feedback controller to regulate gene expression in a microbial consortium. The implementation involves distributing the proportional and derivative control actions between two different cellular populations that can communicate with each other and regulate the output of a third target cellular population. We derive analytical conditions on biological parameters and control gains to adjust the system's static and dynamical properties. We then validate the strategy's performance and robustness through extensive *in silico* experiments.**

I. Introduction

The aim of Synthetic Biology is to engineer biological systems with novel functionalities [1]. This is made possible by designing artificial genetic circuits and embedding them into living cells, such as bacteria or yeast, changing their natural behavior to make them, for example, produce some proteins or other chemicals of interest. Applications range from health treatments [2] to bioremediation [3] and production of drugs or biofuels [4]. However, due to the inherently nonlinear and stochastic nature of the biochemical processes involved, reliable and robust regulation of gene expression must be guaranteed by designing synthetic feedback control architectures. Although the control theoretic literature abounds with high performance, robust control solutions, such as MPC algorithms or discontinuous controllers, the need for implementing the control action using biochemical reactions performed inside the cell strongly limits the possible structure of the controllers that can be realized. Hence, simpler feasible solutions have been proposed in the literature (see [5], [6] for an overview); most notably, the antithetic feedback controller realizing an integral action that guarantees robust perfect adaptation with respect to noise and parameters' uncertainties [7], [8]. Recently, it has been proposed that Proportional-Integral-Derivative (PID) controllers can be implemented via biomolecular reactions and embedded in a single cell to enhance the stability and performance of antithetic controllers, by adding both promptness of regulation response and damping with respect to oscillations [9], [10]. However, in some applications it is more important to avoid oscillations than to ensure a precise regulation, e.g. when engineering the immune response [11]. In these cases a simpler PD control scheme should be preferred because it can guarantee fast and damped regulation of the biological process.

The implementation of biochemical controllers in living cells is also limited by technological and biological constraints, e.g. incompatible chemical reactions, metabolic load or retroactivity [1]. As a consequence, embedding more complex biomolecular controllers consisting of multiple actions (e.g. a PI, PD or PID) inside a single cell can be challenging. A promising solution to these problems is to distribute the control functionalities across different populations in a microbial consortium. The resulting *multicellular* control architecture can both minimize unwanted effects and increase modularity and re-usability of the designed components [1].

In this Letter, we integrate and expand our previous work on multicellular PI controllers [12] by presenting a multicellular PD control strategy where two *controller populations*, each implementing one of the two control actions, regulate a biological process inside a third *target population*, closing the feedback loop by means of diffusing quorum sensing molecules produced by the cells. First, we derive a model of the consortium. Then, we provide some design guidelines for the choice of the control gains based on analytical results, linking the control parameters to the static and dynamical performance of the closed-loop system. The theoretical analysis is complemented with *in silico* experiments carried out via *BSim* [13]. We wish to emphasize that the analysis and design of a fully distributed biomolecular derivative action is a fundamental step together with our previous work in [12] to achieve a fully distributed PID control strategy, which is our ultimate goal.

II. Multicellular PD control strategy

As stated above, the overarching goal of our design is to engineer a multicellular consortium where two controller populations implement the proportional and the derivative control actions needed to realize a strategy similar to the classical PD control strategy [14],

$$u_{PD}(t) := u_P(t) + u_D(t) = k_P e(t) + k_D \dot{e}(t), \qquad (1)$$

where $k_P > 0$ and $k_D > 0$ are the proportional and derivative gains, $e(t)$ is the control error defined as the mismatch between the measured output, say $y(t)$, of the process within a third target population (see Fig. 1) and the desired reference value $Y_{\mathrm{d}}(t)$, provided either externally to the controller cells or hard-coded into them as a constitutive promoter. As in

Vittoria Martinelli and Mario di Bernardo are with the Department of Electrical Engineering and Information Technology, University of Naples Federico II, Naples, Italy (email: vittoria.martinelli@unina.it, mario.dibernardo@unina.it). Davide Salzano is with the Department of Chemical, Materials and Production Engineering (email: davide.salzano@unina.it) and Davide Fiore is with the Department of Mathematics and Applications "R. Caccioppoli" of the same University (email: davide.fiore@unina.it).

The authors wish to acknowledge support from the research project PRIN 2017 - VECTORS funded by the Italian Ministry of University and Research, the Italian PNRR Research project MNESYS and the Italian PNC Research project "Digital Health".

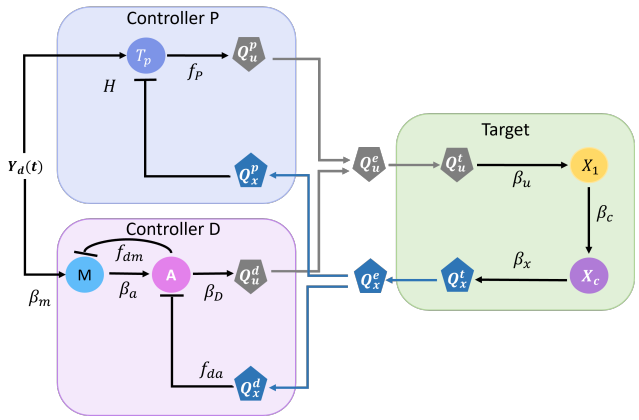

Fig. 1: Abstract implementation of the proposed multicellular PD controller. The controller populations compare the reference signal $Y_{\mathrm{d}}(t)$ and the quorum sensing molecule Q_x, which is produced proportionally to the target gene X_c. The process $\Phi(t)$ is represented by the couple of genes X_1 and X_c, in which X_1 is the actuated by the quorum sensing molecule Q_u. Circles represent internal molecular species, while polygons are the signaling molecules.

[9], here we assume that the desired output, $Y_{\mathrm{d}}(t)$ is either a succession of step functions or some constant value.

The abstract biological implementation of our proposed distributed PD control strategy is shown in Fig. 1. Therein, each controller population computes the control error $e(t)$ by comparing the reference signal $Y_{\mathrm{d}}(t)$ with the measure of the output $y(t)$ corresponding to the expression level of X_c within the target population. Such measure is broadcast to the whole consortium via the quorum sensing molecule Q_x which acts as a proxy for $y(t)$. The control input $u_{PD}(t)$ computed by the two controller populations is delivered to the target cells by means of the quorum sensing molecule Q_u, that is produced by the controllers and effectively serves as the "actuating" signal in this multicellular control scheme. To avoid cross-talking effects [15], Q_x and Q_u are assumed to be orthogonal.

We will show next that the reactions depicted in Fig. 1 implement a distributed biomolecular PD controller.

A. Mathematical Modelling

We derive a model capturing the *aggregate* dynamics of the microbial consortium, that is the evolution of the concentrations of the biochemical species averaged over all cells in a population. (Details on the derivation of the aggregate dynamics from the single cell dynamics are reported in Appendix C.)

As also done in [12], we make the following simplifying assumptions: (i) all populations in the consortium are equally balanced, that is, the three populations are composed by the same number of cells, N; (ii) the total number of cells in the consortium is constant. Note that the former assumption can be achieved by means of external ratiometric controllers, e.g. [16], while the latter assumption is generally verified in experimental environments with limited space and resources, e.g., microfluidics, chemostats, vials. From these assumptions it follows that the diffusion dynamics of the quorum sensing molecules through the cells' membranes can be supposed to have the same diffusion rate η. (This assumption will be relaxed later in Section IV). In what follows, the superscripts e, t, p, d, are used to denote quantities in the "environment", in the "target" cells, in the "proportional", or in the "derivative" controller cells, respectively.

1) Target cells: As done in [7], [9], we assume that the biological process to be controlled inside the target cells consists of only two genes, X_1 and X_c (Fig. 1). The target gene X_c is directly activated by X_1, which in turns is actuated by the quorum sensing molecule Q_u produced by the controller cells. Using mass-action kinetics, the dynamics of the genetic network inside the target cells can therefore be described by the following set of ODEs:

$$\begin{aligned} \dot{X}_1 &= \beta_u Q_u^t - \gamma_1 X_1, \\ \dot{X}_c &= \beta_c X_1 - \gamma_c X_c, \end{aligned} \tag{2}$$

where β_u and β_c are activation rates describing the strength of the transcription factors X_1 and Q_u, while γ_1 and γ_c are degradation rates.

The output of the process, corresponding to the expression level of X_c, is broadcast to the other cells by means of the diffusing quorum sensing molecule Q_x, which is produced by the target cells. Assuming as in [12] that the production of Q_x is proportional to X_c, the dynamics of the sensing molecule inside the target cells is described by:

$$\dot{Q}_x^t = \beta_x X_c + \eta(Q_x^e - Q_x^t) - \gamma_t Q_x^t, \tag{3}$$

where β_x is the activation rate of Q_x, η is the diffusion rate of the molecule across the cell membrane, and γ_t is the dilution rate into the target cells.

2) Proportional controller cells: The Proportional controller is implemented here as in [9] as a nonlinear function $f_P = f_P(Q_x, Y_{\mathrm{d}})$, activating the production of Q_u. Specifically, the dynamics of the concentration of Q_u in the Proportional controllers is given by:

$$\dot{Q}_u^p = \beta_P Y_{\mathrm{d}} \frac{\mu Y_{\mathrm{d}}}{\mu Y_{\mathrm{d}} + \theta Q_x^p} + \eta(Q_u^e - Q_u^p) - \gamma_p Q_u^p, \tag{4}$$

where γ_p is the dilution rate of the quorum sensing molecules into the Proportional cells, μ and θ are positive control parameters, and β_P is a tunable parameter which plays the role of a proportional gain. It has been shown in [9] that the first term in (4) realizes a control action that is a function of the control error $e(t) := \mu Y_{\mathrm{d}} - \theta Q_x$.

3) Derivative controller cells: An approximation of the time derivative of the control error $e(t)$ can be obtained by embedding in the controller population the biomolecular circuit represented in Fig. 1 (see Appendix A for further details), whose dynamics can be described as follows:

$$\begin{aligned} \dot{A} &= \beta_a M - \gamma_a Q_x^d \frac{A}{k_a + A} - \gamma_d A, \\ \dot{M} &= \beta_m Y_{\mathrm{d}} - \gamma_m A \frac{M}{k_m + M}, \end{aligned} \tag{5}$$

where γ_d is the dilution rate of A due to cell growth and division, and β_a and β_m are activation rates, which in turns are actively degraded by Q_x and A, respectively, through enzymatic reactions modeled here via Michaelis-Menten functions with constants γ_a, k_a, γ_m, k_m. For the sake of simplicity, we assumed here that the quorum sensing molecule Q_x also directly acts as a degradation enzyme on A. The derivative control action is then delivered to the targets by means of the quorum sensing molecule Q_u, produced by the controllers at a rate proportional to A (and thus proportional to an approximation of $\dot{e}(t)$), whose concentration inside the controllers is given by:

$$\dot{Q}_u^d = \beta_D A + \eta(Q_u^e - Q_u^d) - \gamma_d Q_u^d, \tag{6}$$

where β_D plays the role of a derivative gain, and the other parameters have an analogous meaning to those in (3).

In addition, the dynamics of Q_x and Q_u into cells where they are not produced is described by:

$$\begin{aligned} \dot{Q}_x^{\mathrm{h}} &= \eta(Q_x^e - Q_x^{\mathrm{h}}) - \gamma_h Q_x^{\mathrm{h}}, \quad \mathrm{h} \in \{p, d\} \\ \dot{Q}_u^t &= \eta(Q_u^e - Q_u^t) - \gamma_t Q_u^t. \end{aligned} \tag{7}$$

Finally, the model is completed by describing the evolution of the concentrations of the quorum sensing molecules into the environment:

$$\begin{aligned} \dot{Q}_x^e &= N\eta \sum_{\mathrm{j}\in\mathcal{S}} (Q_x^{\mathrm{j}} - Q_x^e) - \gamma_e Q_x^e, \\ \dot{Q}_u^e &= N\eta \sum_{\mathrm{j}\in\mathcal{S}} (Q_u^{\mathrm{j}} - Q_u^e) - \gamma_e Q_u^e, \end{aligned} \tag{8}$$

where N is the number of cells in each population (assumed to be balanced), and $\mathcal{S} = \{p, d, t\}$.

III. Design of the microbial consortium

The goal of the multicellular PD architecture shown in Fig. 1 and modelled by (2)-(8) is to regulate the concentration of the quorum sensing molecule Q_x^t, that acts as a proxy of the target output X_c, to the set-point specified via the reference signal Y_{d} with given static and dynamic performance. Specifically, we assume the desired maximum amplitude of the steady state error to be ϵ_e with a settling time less than ϵ_t and an overshoot $s_{\%} \leq \epsilon_s$. Note that these bounds may vary depending on the specific application of interest. Hence, in this work we will not fix these quantities *a priori*. Instead, we will investigate how the control gains can be chosen so as to modulate the settling time, the overshoot and the steady state error that can be achieved.

We will show that, as for the classical PD control, the addition of the derivative action to the consortium can provide a prompter and better regulation of the process output inside the target cells. However, the control gains β_P and β_D in (4) and (6) need to be appropriately tuned to achieve the desired stability and performance. Next, we provide analytical conditions on the control gains that can be used to tune the static precision and the characteristics of the transient response of the closed-loop system, and we compare them to those of the simpler Proportional controller presented in [12].

A. Reduced order model

To derive meaningful analytical conditions we make the following simplifying assumptions, commonly made in the literature, e.g., [9], [12], [17].

Assumptions *The multicellular control system* (2)-(8) *satisfies the following proprieties:*

- A1 *All cell populations grow and divide at the same rate.*
- A2 *The quorum sensing molecules Q_u and Q_x diffuse faster than they degrade.*
- A3 *The enzymatic reactions in* (5) *occur with saturation of the substrates.*
- A4 *The dynamics of the derivative action* (5) *is sufficiently faster than the controlled process in* (2).

Remark 1 *Assumption A1 implies that all cells have the same dilution rate, i.e. $\gamma_1 = \gamma_c = \gamma_p = \gamma_d = \gamma_t = \gamma$, which is a reasonable assumption if all populations are realized using the same biological chassis, and therefore, despite inevitable fluctuations, grow and divide at the same rate. Assumption A2 implies that $\eta \gg \Gamma_{PD}$, with $\Gamma_{PD} := \gamma_p + \gamma_d + \gamma_t + \gamma_e = 3\gamma + \gamma_e$, and it is common in the literature and holds in different models parameterized from in vivo experiments, see e.g. [17]. Assumption A3 is commonly made in the literature (see for example [18]) and it implies that $K_a \ll A$ and $K_m \ll M$ [19]. Assumption A4 allows to perform a time scale separation between the dynamics of the process and the one of the derivative controller, and it can be satisfied by requiring that the frequency content of $X_c(t)$ (and thus of $Q_x(t)$) is bounded by some value $\omega_{\max}$, and the parameters of the derivative motif are chosen accordingly (see [9] and Appendix A for details).*

Under the previous assumptions, the dynamics of the multicellular system can be approximated by the following reduced order model (see Appendix A for details):

$$\begin{aligned} \dot{X}_1 &= -\gamma_1 X_1 + \tfrac{1}{3\gamma}\beta_u \left(\beta_P Y_{\mathrm{d}} \tfrac{3\gamma\mu Y_{\mathrm{d}}}{3\gamma\mu Y_{\mathrm{d}} + \theta\beta_x X_c} + \beta_D A\right), \\ \dot{X}_c &= \beta_c X_1 - \gamma X_c, \end{aligned} \tag{9}$$

with A defined as in (18). Note that the transfer function of system (9) can be locally mapped to the equilibrium point of the closed-loop system to the one of a classic PD controller, see [9] for further details.

B. Static and transient performance

Setting $\dot{X}_1 = 0$ and $\dot{X}_c = 0$ in (9), the equilibria can be obtained as

$$\begin{aligned} \bar{X}_1^{\pm} &= \frac{1}{6}\left(\beta_D\alpha - \delta \pm \sqrt{(\beta_D\alpha + \delta)^2 + \beta_P \tfrac{36\beta_u}{\gamma^2}\delta}\right) Y_{\mathrm{d}}, \\ \bar{X}_c^{\pm} &= \tfrac{\beta_c}{\gamma}\bar{X}_1^{\pm}, \end{aligned} \tag{10}$$

where $\alpha := \frac{\beta_m\beta_u}{\gamma^2\gamma_m}$ and $\delta := \frac{9\gamma^2\mu}{\beta_c\beta_x\theta}$. Since the state variables X_1, X_c describe the concentration of chemical species, we restricted the admissible solutions to be positive. And thus, since $\bar{X}_1^-$ is negative for any positive values of the system parameters, the only admissible equilibrium point is

$(\bar{X}_1^+, \bar{X}_c^+)$, which, by applying the Routh-Hurwitz criterion, can be proved to be locally asymptotically stable for any value of the parameters (see Appendix D for details on the stability analysis).

Next, from the expression of the control error at steady-state (the derivation is omitted here for the sake of brevity), we find that if the control gains are positive ($\beta_P, \beta_D \geq 0$) and such that:

$$\beta_D + \frac{\beta_P}{2}\frac{\gamma_m}{\beta_m} - \frac{9\gamma^4\gamma_m\mu}{\beta_c\beta_u\beta_x\beta_m\theta} = 0, \tag{11}$$

the steady-state error can theoretically be made null provided that all parameters are perfectly known. In practice, this is unrealistic in biological implementations of the controller and therefore the error can only be made small enough by appropriately tuning the gains around the values suggested in (11).

We assess the (local) transient performance by studying the eigenvalues of the linearization of system (9) when (11) is fulfilled about $(\bar{X}_1^+, \bar{X}_c^+)$, where, substituting (11) into (10), $\bar{X}_c^+ = \frac{\Gamma_{PD}}{\beta_x}\frac{\mu Y_\mathrm{d}}{\theta}$. Simple algebraic manipulations yield:

$$\lambda_{PD_{1,2}} = -\rho \pm \sqrt{\rho^2 - \left(\gamma^2 + \frac{\beta_P\beta_c\beta_u\beta_x\theta}{36\gamma^2\mu}\right)}, \tag{12}$$

where $\rho := \gamma + \frac{\beta_D\beta_c\beta_u\beta_x\gamma_a}{18\beta_a\gamma^2\gamma_m}$.
The eigenvalues are therefore both real and negative if:

$$\beta_D \geq 18\frac{\beta_a\gamma^3\gamma_m}{\beta_c\beta_u\beta_x\gamma_a}\left(\sqrt{1 + \frac{\beta_P\beta_c\beta_u\beta_x\theta}{36\gamma^4\mu}} - 1\right), \tag{13}$$

and correspondingly the transient response is characterized by the absence of oscillations, otherwise they are complex conjugates with negative real part.

C. Comparison with the Proportional controller

To highlight the advantages of adding a derivative control action to the multicellular control scheme, we compare the static and transient performances of the PD controller with those of the P controller alone we previously studied in [12].

Regarding the steady-state, also in the case when only a proportional biomolecular controller is present, the error can be made theoretically null (and therefore closer to zero in practice) provided that all the system parameters are perfectly known and the proportional gain is selected about the value [12]:

$$\beta_P^* = \frac{8\gamma^4\mu}{\beta_c\beta_u\beta_x\theta}. \tag{14}$$

Following similar steps as those taken to obtain (12), we find that in the absence of the derivative action when β_P is set as in (14), the transient response is governed by the pair of complex conjugate eigenvalues:

$$\lambda_{P_{1,2}} = -\gamma \pm j\sqrt{\frac{\beta_P\beta_c\beta_u\beta_x\theta}{16\gamma^2\mu}}. \tag{15}$$

Thus, when the derivative action is added to the consortium, if the gains are tuned so that $\lambda_{PD_{1,2}}$ are real, i.e. condition (13) holds, by comparing (12) with (15) we find that the PD strategy can indeed guarantee faster convergence (that is, $|\Re\{\lambda_{P_{1,2}}\}| < \max_i |\Re\{\lambda_{PD_i}\}|$) by further requiring that:

$$\beta_D < \beta_P\frac{\beta_a\gamma_m\theta}{4\gamma\gamma_a\mu}. \tag{16}$$

Also, if $\lambda_{PD_{1,2}}$ are complex conjugate, it is easy to verify that $\Re\{\lambda_{PD}\} < \Re\{\lambda_P\}$ and $\Im\{\lambda_{PD}\} < \Im\{\lambda_P\}$ for any choice of the control gains, therefore, the PD controller always guarantees faster response and more damped oscillations than the Proportional controller alone.

IV. In silico Experiments

We validated the proposed PD multicellular architecture via *in silico* experiments carried out in Matlab and BSim [13] using the model described by equations (2)-(8).

First, we validated the theoretical predictions using Matlab. Specifically, as reported in Fig. 2, we computed for different values of the gains β_P and β_D the overshoot $s_\%$, the 5% settling time $T_{s_{5\%}}$, and the relative percentage steady-state error defined as $\bar{e}_\% = \left|\frac{\bar{Q}_x^t - Q_\mathrm{d}}{Q_\mathrm{d}}\right| \times 100\%$, where $\bar{Q}_x^t$ is the steady-state value of $Q_x^t(t)$ and $Q_\mathrm{d} = \frac{\mu Y_\mathrm{d}}{\theta}$. We found that, as expected from the analysis, the PD strategy can guarantee bounded steady-state error for gains chosen close to the theoretical estimates reported in (11) ($\beta_D < 0.17$, $\beta_P = 0.09 - 0.54\,\beta_D$). For the sake of completeness we also report in Fig. 3 the steady-state error, overshoot and settling time when only the Proportional control action is present ($\beta_D = 0$). Also we notice that, as predicted by (12) and (15), the proportional action used on its own always causes overshoots in the closed-loop response whereas there is a wide range of control parameters (see Fig. 2.b) where the PD action ensures no overshoot. Also, when condition (16) holds ($\beta_D < 4.89\,\beta_P$), the PD architecture provides faster dynamic regulation than the Proportional one (see Fig. 2.c).

We further validated our theoretical results by carrying out agent-based simulations in BSim accounting for cell growth, cell-to-cell variability, diffusion and the geometry of cells and of the hosting chamber. In all the simulations, we set the initial concentration for all chemical species to zero. This emulates an experimental protocol where each cellular population is grown separately from the others prior to the beginning of the experiment. We assumed the cells are growing in a scaled-down version of the microfluidic chamber used in [16], [20]. Specifically, the chamber has dimensions $17\mu\,\mathrm{m} \times 15\mu\,\mathrm{m} \times 1\ \mu\mathrm{m}$ and can host around 100 cells, which is a good compromise between computational time and statistical relevance. Unless otherwise stated, the growth and mechanical parameters of cells and the nominal values of the parameters in the network were chosen as described in Appendix B.

We chose values of the control gains β_P and β_D that were shown in Matlab (see Fig. 2) to guarantee $e_\infty < 20\%$ when $Y_\mathrm{d} = 60\,\mathrm{nM}$ and to also satisfy condition (16). We ran 10 agent-based simulations, each time randomly selecting the control gains with uniform distribution and evaluating the performance. Figure 4 shows that both the P and PD architectures have good regulation capabilities. Moreover, it confirms that on average the addition of a derivative action

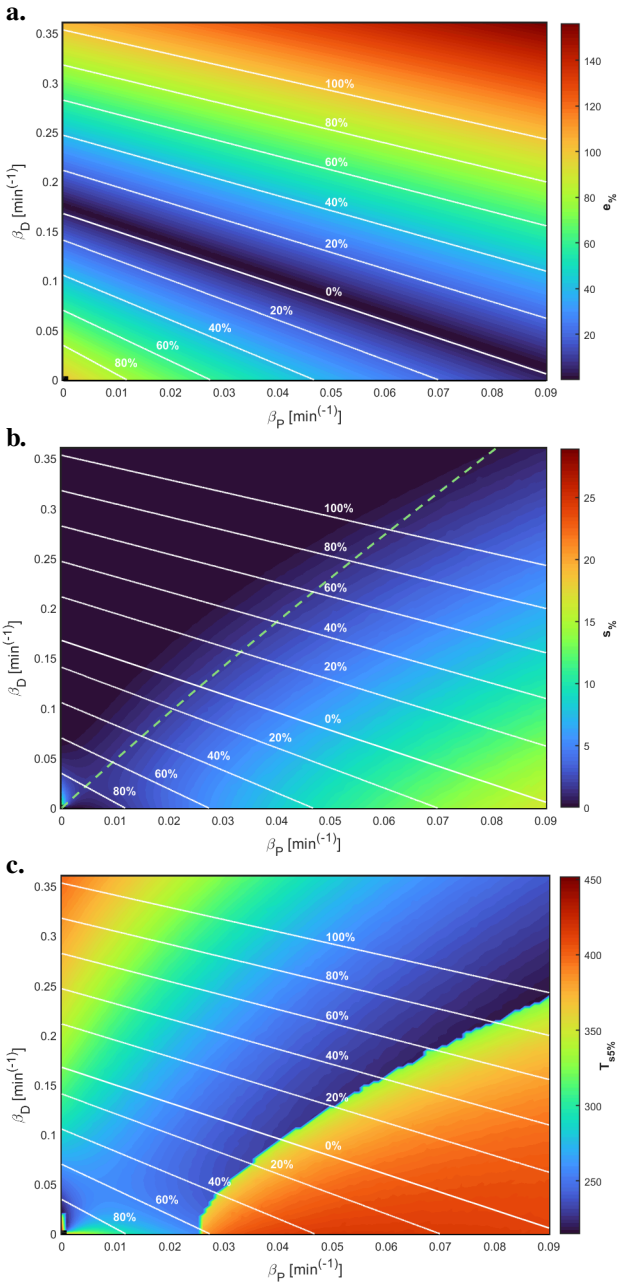

Fig. 2: *In silico* experiments in Matlab: percentage error $e_{\%}$ (a), percentage overshoot $s_{\%}$ (b) and settling time $T_{s_{5\%}}$ (c) when the targets are controlled by the PD controller. The control gains β_P and β_D were varied in the intervals $[0, 0.09]$ and $[0, 0.36]$ with step size equal to $0.0009\,\mathrm{min}^{-1}$ and $0.0036\,\mathrm{min}^{-1}$, respectively. The reference signal was set to $Y_{\mathrm{d}} = 60\,\mathrm{nM}$ in all simulations. The white isoclines bound the regions in the parameters' space (β_P, β_D) with the same upper bound on the percentage error. The 0% isocline in panel (a) is the analytical estimate given by (11) while the green dashed line in panel(b) represents the condition to have real eigenvalues given by equation (13).

consistently reduces the overshoot (9.76% for the PD, and 18.29% for the P controller). Instead, the reduction of the settling time was just about 10% (about 355 min for the PD, and 392 min for the Proportional). As for the steady-state error (4.55% for the PD, and 2.71% for the Proportional), the difference between the two strategies was negligible.

Finally, we tested the robustness of the P and PD strategies

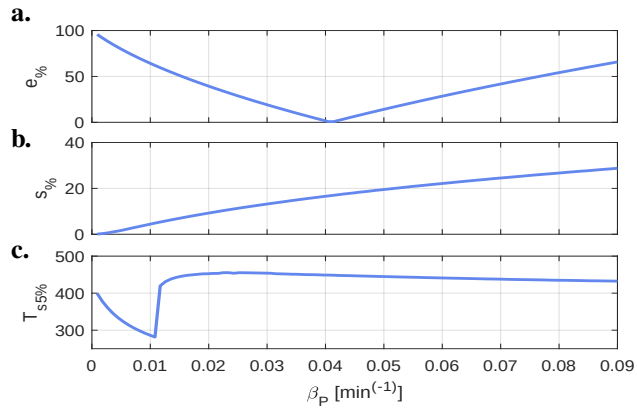

Fig. 3: Proportional performance validation in Matlab: percentage error $e_{\%}$ (a), percentage overshoot $s_{\%}$ (b) and settling time $T_{s_{5\%}}$ (c) when the targets are controlled by a proportional controller. The control gain was varied in the interval $[0, 0.09]$ with step size equal to $0.0009\,\mathrm{min}^{-1}$. The reference signal was set to $Y_{\mathrm{d}} = 60\,\mathrm{nM}$ in all simulations.

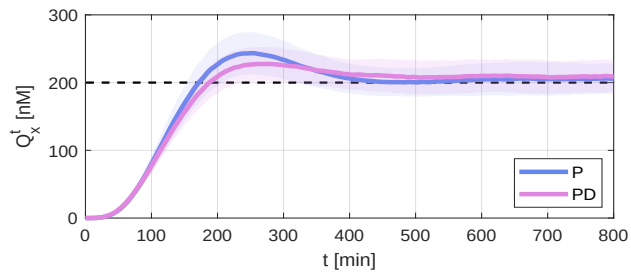

Fig. 4: Control performance validation in BSim: mean (continuous line) and standard deviation (shaded area) of the average concentration of Q_x^t in the targets. The statistics were computed over 10 simulations. The blue lines are obtained using a Proportional controller and the purple ones using a PD controller. Control gains were drawn with uniform distribution from the region of the parameter space (β_P, β_D) in Figure 2 in which $\bar{e}_{\%} < 20\%$. For the PD architecture we also imposed condition (16). The reference signal $Q_{\mathrm{d}} = \mu Y_{\mathrm{d}}/\theta$ is depicted as a dashed line. At $t = 0\,\mathrm{min}$, 18 cells, equally divided between the populations, were positioned at the center of the chamber along a horizontal stripe.

as the cell-to-cell variability increases in the cell populations. We modeled this effect by drawing, at cell division, each parameter of the daughter cells, say ρ, from a normal distribution centered at its nominal value $\hat{\rho}$ with standard deviation $\sigma = CV \cdot \hat{\rho}$, where CV is the coefficient of variation. We compared the robustness of the two architectures, as the CV increases, by evaluating the settling time, the overshoot, and the average relative percentage steady-state error, defined as $e_{\%} = \frac{1}{n}\sum_{k=1}^{n}\left|\frac{\hat{Q}_x^t - Q_{\mathrm{d}}}{Q_{\mathrm{d}}}\right| \times 100\%$, where $\hat{Q}_x^t$ is the value of $Q_x^t(t)$, averaged over the last 200 min, of the k-th experiment, $Q_{\mathrm{d}} = \frac{\mu Y_{\mathrm{d}}}{\theta}$, and n is the total number of experiments we conducted for each value of CV. Fig. 5 shows that the P and the PD strategies both possess good robustness (the steady-state error never exceeds 20%). We observe that while the Proportional controller guarantees a lower residual error under perturbations (Fig. 5.a), the PD control strategy reduces the overshoot even in the presence of high cell-to-cell variability (Fig. 5.c); no significant difference between the two being detected in terms of settling time (Fig. 5.b).

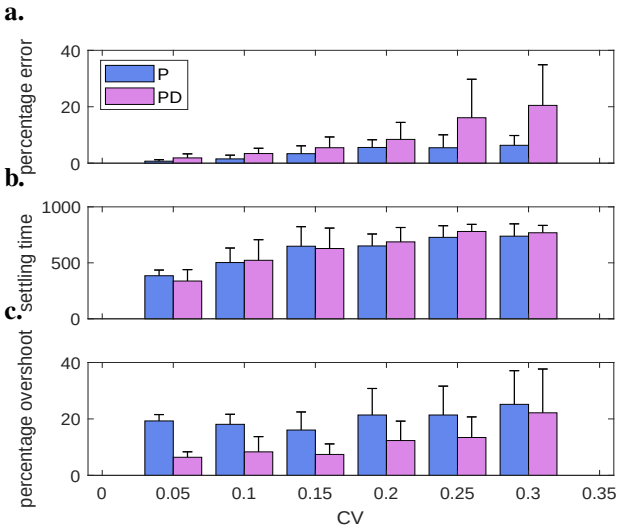

Fig. 5: Sensitivity to parameter variations: mean and standard deviation of the percentage of error at steady-state (a), settling time (b) and overshoot (c) as the cell-to-cell variability increases. Blue bars are obtained using only a Proportional controller and purple bars when a PD controller was employed. For each value of $CV \in \{0.05, 0.1, 0.15, 0.2, 0.25, 0.3\}$ we performed $n = 50$ simulations drawing independently cells' parameters from a normal distribution centered at their nominal value $\hat{\rho}$ with standard deviation $\sigma = CV \cdot \hat{\rho}$. The reference signal was set to $Y_{\mathrm{d}} = 60\,\mathrm{nM}$, while the gains were chosen as $\beta_P = 0.0414\,\mathrm{min}^{-1}$ and $\beta_D = 0.0933\,\mathrm{min}^{-1}$. All simulations were performed for a total time of $800\,\mathrm{min}$.

V. Conclusions

We discussed the implementation of a distributed biomolecular PD controller. Analytical conditions were derived for control gains to achieve the desired performance. It was shown that the derivative action helps reduce overshoots and settling time. Numerical and *in silico* experiments were conducted to confirm the effectiveness of the proposed strategy, despite cell-to-cell variability and other realistic effects. Future work involves exploiting the results presented here with our previous results in [12] to achieve a fully distributed biomolecular PID controller.

Appendix

A. Derivation of the reduced order model (9)

Under Assumption A2, we can assume that the quorum sensing molecules are always at steady state. Therefore, by imposing that $\dot{Q}^j_{\mathrm{h}} = 0$ and $\dot{Q}^e_{\mathrm{h}} = 0$, with $\mathrm{h} \in \{u, x\}$ and $j \in \mathcal{S}$, where $\mathcal{S} = \{t, p, d\}$, and under the hypothesis of a large number of cells, after some algebra we have that:

$$\begin{aligned} Q^j_x &\approx Q^e_x = Q_x = \frac{1}{3\gamma}\beta_x X_c, \\ Q^j_u &\approx Q^e_u = Q_u = \frac{1}{3\gamma}\left(\beta_P Y_{\mathrm{d}} \tfrac{\mu Y_{\mathrm{d}}}{\mu Y_{\mathrm{d}} + \theta Q_x} + \beta_D A\right). \end{aligned} \tag{17}$$

Under Assumption A4 there exists some $\omega_{\max}$ upper bounding the frequency contents of $Q_x(t)$, therefore, if the parameters of the derivative motif are chosen so as to satisfy the condition $\beta_a \gamma_m \gg |\omega^2_{\max} + \gamma_0 \omega_{\max}|$, then A in (5) contains an approximation of the derivative of the control error $e(t)$ given by (see [9] for further details):

$$A \approx -\frac{1}{3\gamma}\frac{\gamma_a \beta_x}{\beta_a \gamma_m}\dot{X}_c + \frac{\beta_m}{\gamma_m}Y_{\mathrm{d}} = \frac{\gamma_a}{\beta_a \gamma_m \theta}\dot{e}(t) + \frac{\beta_m}{\gamma_m}Y_{\mathrm{d}}. \tag{18}$$

This is because, under Assumption A2 we can substitute the expression of Q_x at steady-state in (17) in the control error $e(t)$. Then, assuming a constant reference signal Y_{d} and taking the time derivative of $e(t)$, yields:

$$\dot{e}(t) = -\theta \frac{\beta_x}{3\gamma}\dot{X}_c. \tag{19}$$

Combining the quorum sensing steady-state expressions in (17) and (18) with (2) we then obtain the reduced model (9).

B. Nominal biochemical parameters

The growth and mechanical parameters used in the BSim simulations were selected as in [17], while the nominal biochemical parameters were chosen as: $\beta_u = 0.06\,\mathrm{min}^{-1}$, $\beta_x = 0.03\,\mathrm{min}^{-1}$, $\gamma = 0.023\,\mathrm{min}^{-1}$, $\eta = 2\,\mathrm{min}^{-1}$ (taken from [17]); $\beta_c = 0.1\,\mathrm{min}^{-1}$, $\mu = 1\,\mathrm{min}^{-1}$, $\theta = 0.3\,\mathrm{min}^{-1}$, $\beta_a = 1.5\,\mathrm{min}^{-1}$, $\beta_m = 0.4167\,\mathrm{min}^{-1}$, $\gamma_a = \gamma_m = 1.5\,\mathrm{min}^{-1}$ (taken from [9]); $\gamma_e = 0.0023\,\mathrm{min}^{-1}$.

C. Derivation of the aggregate model

Here we present the derivation of the aggregate model reported in Section II-A that describes the evolution of the average concentrations of chemical species in the whole consortium. For the sake of brevity, we report there only the case of a consortium comprising Proportional controller cells and target cells. The case of three populations, in which also the derivative controller population is present, follows straightforwardly. The aggregate dynamics of the non-diffusive species (i.e., X_1 and X_c in the target cells, and A and M in the derivative controller cells) follows directly from the single cell model by assuming that the average concentrations follow the same dynamics. For what concerns the diffusive species (i.e., Q_x and Q_u), under the assumptions made in Section III-A, their dynamics inside each cell in the consortium and into the environment is given as (we report here only the dynamics of Q_x for the sake of brevity, a similar analysis follows for Q_u):

$$\dot{Q}^t_{x,k} = \beta_x X_{c,k} + \eta(Q^e_x - Q^t_{x,k}) - \gamma Q^t_{x,k}, \tag{20}$$

$$\dot{Q}^p_{x,i} = \eta(Q^e_x - Q^p_{x,i}) - \gamma Q^p_{x,i}, \tag{21}$$

$$\dot{Q}^e_x = \eta \sum_{\mathrm{j} \in \mathcal{S}} \sum_{k=1}^{N_j} (Q^j_{x,k} - Q^e_x) - \gamma_e Q^e_x, \tag{22}$$

where $X_{c,k}$ and $Q^t_{x,k}$ are the concentrations of the species X_c and Q_x inside the k-th cell of the target population, $Q^p_{x,i}$ is the concentration of the signaling molecule Q_x in the i-th cell embedding the Proportional controller, and Q^e_x is the concentration of Q_x into the environment. Moreover, $\mathcal{S} = \{t, p\}$, and N_t and N_p are the number of cells in the target and Proportional controller populations, respectively. Now, defining $Q^j_x = \frac{1}{N_j}\sum_{k=1}^{N_j} Q^j_{x,k}$ for $j \in \mathcal{S}$ and $X_c =$

$\frac{1}{N_t}\sum_{k=1}^{N_t} X_{c,k}$, we can derive the evolution of the average concentration of Q_x inside each cell population as:

$$\begin{aligned}\dot{Q}_x^t &= \beta_x X_c + \eta(Q_x^e - Q_x^t) - \gamma Q_x^t,\\ \dot{Q}_x^p &= \eta(Q_x^e - Q_x^p) - \gamma Q_x^p.\end{aligned} \tag{23}$$

In addition, we can recast equation (22) as:

$$\begin{aligned}\dot{Q}_x^e &= \eta \sum_{\mathrm{j}\in\mathcal{S}} \left(\sum_{k=1}^{N_j} Q_{x,k}^j - N_j Q_x^e \right) - \gamma_e Q_x^e = \\ &= \eta \sum_{\mathrm{j}\in\mathcal{S}} N_j \left(Q_x^j - Q_x^e \right) - \gamma_e Q_x^e,\end{aligned} \tag{24}$$

and thus, assuming $N_t = N_p = N$, that is, the two populations are balanced, equation (24) becomes:

$$\dot{Q}_x^e = N\eta \sum_{\mathrm{j}\in\mathcal{S}} (Q_x^{\mathrm{j}} - Q_x^e) - \gamma_e Q_x^e. \tag{25}$$

D. Stability analysis of the PD control model

The local stability of system (9) can be assessed by computing the characteristic polynomial linearized about the admissible equilibrium point $(\bar{X}_1^+, \bar{X}_c^+)$ (10), and applying the Routh-Hurwitz criterion [21]. For a second order system the Routh table is given by:

$$\begin{array}{c|cc} s^2 & a_2 & a_0 \\ s^1 & a_1 & 0 \\ s^0 & b_1 & \end{array} \tag{26}$$

The elements in table (26) are computed starting from the coefficients of the characteristic polynomial:

$$p(s) = a_2 s^2 + a_1 s + a_0 \tag{27}$$

For the system in exam, they can be formalized as

$$\begin{aligned} a_2 &= 1,\\ a_1 &= 2\gamma + \frac{\beta_D\beta_c\beta_u\beta_x\gamma_a}{9\beta_a\gamma^2\gamma_m},\\ a_0 &= \gamma^2 + \frac{\omega\gamma^2}{(\phi + \sqrt{\phi^2+\omega})^2},\\ b_1 &= a_0.\end{aligned} \tag{28}$$

where $\omega := 36\beta_P\beta_c\beta_u\beta_x\gamma^4\gamma_m^2\mu\theta$ and $\phi := 9\gamma^4\gamma_m\mu + \beta_D\beta_c\beta_u\beta_x\beta_m\theta$. Since all the parameters of the system are assumed to be positive constants, all the coefficients in equation (28) are positive. As a consequence, no sign permutations happen in the first column of (26) and, applying the Routh-Hurwitz criterion, we can infer that the equilibrium point is locally asymptotically stable.

References

[1] D. Del Vecchio, *et al.*, "Control theory meets synthetic biology," *Journal of The Royal Society Interface*, vol. 13, no. 120, p. 20160380, 2016.

[2] X. Tan, *et al.*, "Synthetic biology in the clinic: engineering vaccines, diagnostics, and therapeutics," *Cell*, vol. 184, no. 4, pp. 881–898, 2021.

[3] E. L. Rylott *et al.*, "How synthetic biology can help bioremediation," *Current Opinion in Chemical Biology*, vol. 58, pp. 86–95, 2020.

[4] Y. Yang, *et al.*, "Plant synthetic biology innovations for biofuels and bioproducts," *Trends in Biotechnology*, vol. 40, no. 12, pp. 1454–1468, 2022.

[5] I. Ruolo, *et al.*, "Control engineering meets synthetic biology: Foundations and applications," *Current Opinion in Systems Biology*, vol. 28, no. 100397, p. 100397, 2021.

[6] M. H. Khammash, "Cybergenetics: Theory and applications of genetic control systems," *Proceedings of the IEEE*, vol. 110, no. 5, pp. 631–658, 2022.

[7] C. Briat, *et al.*, "Antithetic integral feedback ensures robust perfect adaptation in noisy biomolecular networks," *Cell Systems*, vol. 2, no. 1, pp. 15–26, 2016.

[8] M. H. Khammash, "Perfect adaptation in biology," *Cell Systems*, vol. 12, no. 6, pp. 509–521, 2021.

[9] M. Chevalier, *et al.*, "Design and analysis of a proportional-integral-derivative controller with biological molecules," *Cell Systems*, vol. 9, no. 4, pp. 338–353, 2019.

[10] E. Alexis, *et al.*, "On the design of a PID bio-controller with set point weighting and filtered derivative action," *IEEE Control Systems Letters*, vol. 6, pp. 3134–3139, 2022.

[11] P. Wei, *et al.*, "Bacterial virulence proteins as tools to rewire kinase pathways in yeast and immune cells," *Nature*, vol. 488, no. 7411, pp. 384–388, 2012.

[12] V. Martinelli, *et al.*, "Multicellular PI control for gene regulation in microbial consortia," *IEEE Control Systems Letters*, vol. 6, pp. 3373–3378, 2022.

[13] A. Matyjaszkiewicz, *et al.*, "Bsim 2.0: an advanced agent-based cell simulator," *ACS Synthetic biology*, vol. 6, no. 10, pp. 1969–1972, 2017.

[14] K. J. Aström *et al.*, *Feedback Systems. An Introduction for Scientists and Engineers*. Princeton Univ Pr, 2008.

[15] N. Kylilis, *et al.*, "Tools for engineering coordinated system behaviour in synthetic microbial consortia," *Nature communications*, vol. 9, no. 1, p. 2677, 2018.

[16] D. Salzano, *et al.*, "Ratiometric control of cell phenotypes in monostrain microbial consortia," *Journal of the Royal Society Interface*, vol. 19, no. 192, p. 20220335, 2022.

[17] D. Fiore, *et al.*, "Multicellular feedback control of a genetic toggle-switch in microbial consortia," *IEEE Control Systems Letters*, vol. 5, no. 1, pp. 151–156, 2020.

[18] W. Ma, *et al.*, "Defining network topologies that can achieve biochemical adaptation," *Cell*, vol. 138, no. 4, pp. 760–773, 2009.

[19] L. Michaelis, *et al.*, "Die kinetik der invertinwirkung," *Biochem. Z.*, vol. 49, no. 333-369, p. 352, 1913.

[20] B. Shannon, *et al.*, "In vivo feedback control of an antithetic molecular-titration motif in escherichia coli using microfluidics," *ACS Synthetic Biology*, vol. 9, no. 10, pp. 2617–2624, 2020.

[21] J. F. de Cañete, *et al.*, *Automatic Control Systems in Biomedical Engineering: An Interactive Educational Approach*. Springer International Publishing, 2018.